Proceedings of the
Annual Stability Conference
Structural Stability Research Council
Nashville, Tennessee, March 24-27, 2015

Linear Stability Analysis of Steel Thin-Walled Members Through a Higher Order Beam Theory

Ricardo F. Vieira[1], Francisco B. E. Virtuoso[2], Eduardo B. R. Pereira[3]

Abstract
A higher order beam model for the buckling analysis of thin-walled structures is presented. The model relies on the enrichment of the displacement field so as to accurately represent the three-dimensional behaviour of thin-walled structures. The definition of an uncoupled set of deformation modes allows a meaningful definition of hierarchical higher order solutions, which are useful for the linear buckling analysis of thin-walled structures. A criterion for the definition of local and global buckling modes, as well as the possible interaction between modes is put forward. A comparison between the results obtained with the higher order beam model and results obtained from a shell finite element model implemented in ABAQUS allows to conclude not only the efficiency of the beam model but also its simplicity of use.

1. Introduction

Thin-walled structures are prone to both local and global buckling phenomena, being the design of this type of structures often determined by the interaction between theses modes. The stability analysis by a shell finite element model is a standard and accurate procedure to evaluate bifurcation loads and the corresponding buckling modes. Nonetheless, shell finite models can pose certain difficulties in the interpretation of buckling phenomena, particularly when interaction between modes occurs.

Alternatively to shell models, beam models can also be efficiently adopted to perform a stability analysis of a thin-walled structure, having the advantage of allowing a more clear insight into the buckling phenomena. To this end, the beam model has to be capable of reproducing the 3D structural behaviour of the thin-walled structure, namely the corresponding out of plane warping and the in-plane flexure of a cross-section. Moreover, the beam model should be able of providing sets of uncoupled solutions for the stability of the thin-walled structure so as to clearly identify the most relevant buckling modes.

Although considering different approaches, several beam models have been successfully adopted to model thin-walled structures. Essentially, these one-dimensional models rely on the

[1] Assistant Professor, University of Lisbon, <ricardo.figueiredo.vieira@tecnico.ulisboa.pt>
[2] Associate Professor, University of Lisbon, <francisco.virtuoso@tecnico.ulisboa.pt >
[3] Associate Professor, University of Lisbon, <eduardo.pereira@tecnico.ulisboa.pt >

enrichment of the displacement field over the cross-section in order to enhance the accuracy of the model. The quantification of the Saint-Venant principle has been adopted in the formulation of beam models by defining the three-dimensional continuum mechanics in terms of higher order modes, (Genoese 2013, 2014a and 2014b; Ferradi 2013 and 2014). The displacement field of beam models has also been enhanced by adopting (i) an asymptotical analysis of the cross-section (Hodges 2006; Yu 2012); (ii) an approximation through a Taylor's expansion, (Carrera 2010 and 2011) and (iii) an approximation of the displacement field on the beam cross-section by a set of linearly independent basis functions, (Razaqpur 1991; Prokic 1996; Kim 1999; Kim 2000; Kim 2002; Pavaaza 2005; Sadée 2006 and Fatmi 2007).

The so-called generalised beam theory (GBT), which has been developed from the seminal work of (Schardt 1989) towards its applicability to more generic cross-section midline geometries, (Dinis 2006; Gonçalves 2009; Nedelcu 2010; Ranzi 2011 and Ranzi 2014; Jonsson 2011; Andreassen 2013) is a successful theory for the analysis of thin-walled structures; the GBT owes its success to its modal uncoupled nature, which renders the theory an adequate tool for the buckling analysis of thin-walled structures.

Thin-walled structures have also been analyzed through a semi-analytical finite strip analysis (the constrained finite strip analysis - cFSM), being the corresponding mechanical behaviour evaluated through the separation of the corresponding deformation modes, (Li 2011 and Adany, 2008). A comparison between the modal approaches of GBT and cFSM has been presented in (Adany 2009).

The higher order beam model that considers the out of plane warping and the in-plane flexure of thin-walled structures presented in (Vieira 2014) has been applied to the buckling analysis of thin-walled structures. The model copes with the loss of accuracy inherent from the reduction of a three-dimensional elasticity formulation to a one-dimensional model by an enrichment of the beam displacement field on the beam cross-section through the adoption of a set of interpolation functions of a suitable degree, defined over a sufficiently refined mesh of the cross-section. The beam governing equations are derived considering the approximation scheme adopted for the displacement, yielding a set of fourth order differential system of equations. The solution of this system is analyzed through the corresponding non-linear eigenvalue problem, which allows to obtain a set of uncoupled deformation modes.

2. Higher Order Thin-Walled Beam Model

A beam model derived by considering an enriched approximation of the displacement field so as to accurately represent the 3D structural behaviour of a thin-walled structure is considered. The model relies on the approximation of the displacement field on the cross-section by a set of linearly independent basis functions and on a criterion to uncouple the corresponding governing equations for an efficient analysis of thin-walled structures.

The cross-section is divided into elements for the approximation of the displacement field, being each displacement component interpolated independently along each element. A global approximation function, at a cross-section level, is then obtained by ensuring compatibility

between elements. The enrichment of the cross-section displacement field allows a beam model to reproduce the structure three-dimensional behaviour.

However, for the beam model to be efficiently adopted, an uncoupling of the corresponding governing equations, allowing to identify uncoupled structural phenomena, is a key feature. To this end, a set of modes representing the cross-section deformation is derived from the homogeneous solution of the corresponding beam differential equilibrium equations.

The classic equations are retrieved side by side with a set of governing equations representing higher order deformations. Given the procedure adopted for the approximation of the displacement field, the shear deformation of the middle surface in naturally included and the model is applicable to cross-sections with a generic geometry, e.g. open, closed and with more that two non-aligned walls intersecting a cross-section mode.

2.1 Formulation

This formulation considers a cross-section represented by a set of rectilinear wall segments, which form a generic shape, either of open or closed profile. A rectilinear segment can be divided into several elements for better approximation features. Each element is considered to have both a flexural and a membrane structural behaviour. For the flexural behaviour, it is assumed that the elements are sufficiently "thin" in order to consider valid the *Kirchhoff* formulation and hence neglect the shear deformation on the planes perpendicular to the middle surface. The displacement field considering both the membrane and the flexural structural behaviour of the plate is defined as follows:

$$u_x(x,s,n) = \bar{u}_x(x,s) - n\frac{\partial u_n}{\partial x} \tag{1}$$

$$u_s(x,s,n) = \bar{u}_s(x,s) - n\frac{\partial u_n}{\partial s} \tag{2}$$

$$u_n(x,s,n) = \bar{u}_n(x,s) \tag{3}$$

where x represents the beam axis; s the coordinate along the cross-section profile and n the corresponding perpendicular coordinate; $u_x(x,s)$ and $u_s(x,s)$ represent the in-plane displacements associated with the plate membrane behaviour and $u_n(x,s,n)$, the plate transverse displacement, which is considered to be constant over the plate element thickness.

The displacement field of the cross-section middle surface is thus approximated independently in the three spatial directions through the following expressions,

$$\begin{aligned} &\bar{u}_x(x,s) = \boldsymbol{\phi}^t\,\mathbf{u}_x, \quad \bar{u}_s(x,s) = \boldsymbol{\psi}^t\,\mathbf{u}_s \quad \text{and} \\ &\bar{u}_n(x,s) = \boldsymbol{\chi}^t\,\mathbf{u}_n \end{aligned} \tag{4}$$

where $\boldsymbol{\phi}, \boldsymbol{\psi}$ and $\boldsymbol{\chi}$, correspond to the sets of the adopted basis functions; the basis functions are defined by assembling the approximation of the displacement field over each thin-walled element. The presented model was derived considering the approximation of the displacement field over the beam cross-section through a set of globally defined basis functions. However, it is more versatile, and computationally more efficient, to divide the cross-section into a set of rectilinear laminar elements, forming a cross-section mesh, and to consider an approximation for the displacement field defined over each thin-walled element.

The assemblage of the cross-section "elements" is made by considering the compatibility in terms of the middle surface displacements at the corresponding end-sections of the elements, neglecting the compatibility of the displacement field along the thin-wall thickness. The approximation functions at the element level are required to have a sufficient continuity condition in order to allow the establishment of the beam differential equations.

The degrees of freedom of the thin-walled element with the corresponding approximation functions are represented for an element in Fig.1. A discretization into those elements is performed for the cross-section analysis, within the beam model formulation framework, by considering a suitable mesh without any restrictions regarding its definition; hence, not only any arbitrary polygonal geometry can be considered, but also an *h*-refinement of a rectilinear segment is possible.

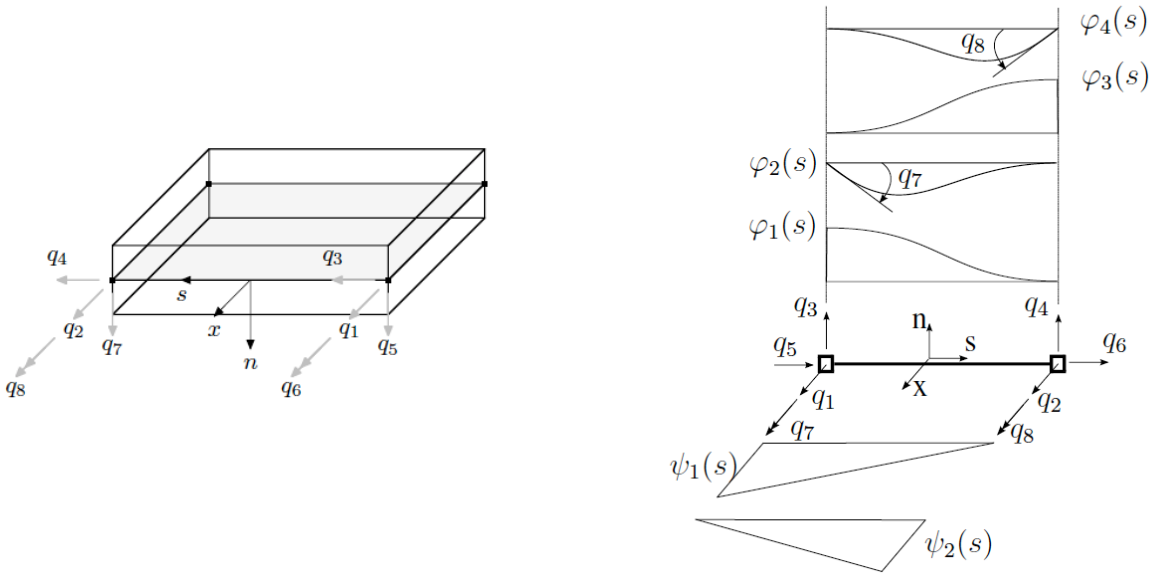

Figure 1: Thin-walled element.

A complete kinematical description for the thin-walled structure is obtained by substituting the approximations made in Eqs. 4 into the displacement field definition given by Eqs 1-3, being written as follows:

$$\begin{aligned} u_x(x,s,n) &= \boldsymbol{\phi}^t\,\mathbf{u}_x - n\,\boldsymbol{\chi}^t\,\mathbf{u}'_n \\ u_s(x,s,n) &= \boldsymbol{\psi}^t\,\mathbf{u}_s - n\,\boldsymbol{\chi}^t_{,s}\mathbf{u}_n \\ u_n(x,s,n) &= \boldsymbol{\chi}^t\,\mathbf{u}_n \end{aligned} \tag{5}$$

The deformation field is obtained under the small displacements hypothesis through the Cauchy infinitesimal compatibility operator by considering the displacement field approximation obtained through Eq. 4, being the corresponding components written as follows,

$$\begin{aligned}
\epsilon_x(x,s,n) &= \frac{\partial u_x}{\partial x} = \boldsymbol{\phi}^t\,\mathbf{u}'_x - n\,\boldsymbol{\chi}^t\,\mathbf{u}''_n \\
\epsilon_s(x,s,n) &= \frac{\partial u_s}{\partial s} = \boldsymbol{\psi}^t_{,s}\,\mathbf{u}_s - n\,\boldsymbol{\chi}^t_{,ss}\,\mathbf{u}_n \\
\gamma_{xs}(x,s,n) &= \frac{\partial u_x}{\partial s} + \frac{\partial u_s}{\partial x} = \boldsymbol{\psi}^t\,\mathbf{u}'_s + \boldsymbol{\phi}^t_{,s}\,\mathbf{u}_x - 2\,n\,\boldsymbol{\chi}^t_{,s}\,\mathbf{u}'_n
\end{aligned} \tag{6}$$

The corresponding stress field can be obtained through the constitutive relation,

$$\boldsymbol{\sigma} = \mathbf{C}\,\boldsymbol{\epsilon} \quad \text{with} \quad \boldsymbol{\sigma} = [\sigma_x(x,s,n) \quad \sigma_s(x,s,n) \quad \sigma_{xs}(x,s,n)]^t \tag{7}$$

where the constitutive matrix $\mathbf{C}$ is defined for a plane stress of each wall considering a plate flexural behaviour. The stress field is obtained by considering the constitutive relation of Eq. 7 and the strain field given by Eqs. 6, being written in terms of the displacement field as follows,

$$\begin{aligned}
\sigma_x(x,s,n) &= E^*\left(\boldsymbol{\phi}^t\,\mathbf{u}'_x + \nu\,\boldsymbol{\psi}^t_{,s}\,\mathbf{u}_s\right) - n\,E^*\left(\boldsymbol{\chi}^t\,\mathbf{u}''_n + \nu\,\boldsymbol{\chi}^t_{,ss}\,\mathbf{u}_n\right) \\
\sigma_s(x,s,n) &= E^*\left(\boldsymbol{\psi}^t_{,s}\,\mathbf{u}_s + \nu\,\boldsymbol{\phi}^t\,\mathbf{u}'_x\right) - n\,E^*\left(\boldsymbol{\chi}^t_{,ss}\,\mathbf{u}_n + \nu\,\boldsymbol{\chi}^t\,\mathbf{u}''_n\right) \\
\sigma_{xs}(x,s,n) &= G\left(\boldsymbol{\psi}^t\,\mathbf{u}'_s + \boldsymbol{\phi}^t_{,s}\,\mathbf{u}_x\right) - 2\,n\,G\,\boldsymbol{\chi}^t_{,s}\,\mathbf{u}'_n
\end{aligned} \tag{8}$$

The vector of generalised forces distributed along the beam axis is written as follows,

$$\mathbf{p} = [\mathbf{p}_x(x) \quad \mathbf{p}_s(x) \quad \mathbf{p}_n(x)]^t \tag{9}$$

where the corresponding components are given by,

$$\begin{aligned}
\mathbf{p}_x(x) &= \int_\Gamma \boldsymbol{\phi}\,f_x(x,s)\,d\Gamma \quad \mathbf{p}_s(x) = \int_\Gamma \boldsymbol{\psi}\,f_s(x,s)\,d\Gamma \\
\mathbf{p}_n(x) &= \int_\Gamma \left[\boldsymbol{\chi}\,f_n(x,s) - \frac{\partial \tilde{m}_{xs}}{\partial s} - \frac{\partial \tilde{m}_x}{\partial x}\right] d\Gamma
\end{aligned} \tag{10}$$

The distributed forces are defined by a set of vectors that gather the corresponding densities defined on the thin-walled middle surface (x, s), which are written as,

$$\begin{aligned}
\mathbf{f} &= \left[\; f_x(x,s) \quad f_s(x,s) \quad f_n(x,s) \;\right]^t \\
\tilde{m}_{xs} &= -n\,\boldsymbol{\chi}_{,s}\,f_s \quad \text{and} \quad \tilde{m}_x = -n\,\boldsymbol{\chi}\,f_x
\end{aligned} \tag{11}$$

Considering the stress and deformation field defined in Eqs. 6 and 8 and by making use of the virtual work principle, a system of equilibrium equations written in terms of displacements is obtained, which can be compactly written as follows:

$$\mathbb{K}_4\,\mathbf{u}'''' + \mathbb{K}_2\,\mathbf{u}'' + \mathbb{K}_1\,\mathbf{u}' + \mathbb{K}_0\,\mathbf{u} - \mathbf{p} = 0 \quad \text{with} \quad \mathbf{p} = \left[\; \mathbf{p}_x \quad \mathbf{p}_s \quad \mathbf{p}_n \;\right]^t \tag{12}$$

Details of the definition of the coefficient matrices in Eq. 12 can be found in (Vieira 2014).

2.3 Linear stability analysis

The higher order thin-walled beam model presented in section 2.2 is adopted for a linear stability analysis of thin-walled structures, allowing to obtain the corresponding local and global bifurcation loads. In fact, the higher order model can adequately consider local buckling phenomena in as much as it is properly enriched so as to accurately represent the cross-section in-plane deformation, (Vieira 2014). Moreover, the criterion adopted for the definition of the uncoupled deformations modes enhances the perception of the thin-walled structural behaviour,

throwing a light into the buckling phenomena. Conversely, a shell finite element model allows to accurately evaluate the buckling phenomena, being however difficult to separately identify the interaction between buckling modes. The capability of the higher order model to consider the behaviour of thin-walled structures by a set of uncoupled deformation modes proves to be an efficient and accurate way of evaluating buckling phenomena, identifying local and global buckling modes, as well as the corresponding couplings.

Towards a buckling analysis, the thin-walled structure is subjected to a set of in-plane stresses at both the end sections, being admitted a linear pre-buckling state of stress, i.e., the displacement field that represents the fundamental path is linearly dependent of a load parameter. The displacement field is obtained from the model governing equations, Eqs. 12, being written as follows:

$$u_{x,f} = \boldsymbol{\phi} \cdot \mathbf{u}_{x,f} \qquad u_{s,f} = \boldsymbol{\psi} \cdot \mathbf{u}_{s,f} \qquad u_{n,f} = \boldsymbol{\chi} \cdot \mathbf{u}_{n,f} \tag{13}$$

The corresponding stress field is given by the following expressions,

$$\begin{aligned} \sigma_{x,f}(x,s,n) &= E^* \, \boldsymbol{\phi} \cdot \mathbf{u}'_{x,f} \\ \sigma_{s,f}(x,s,n) &= E^* \boldsymbol{\psi}_{,s} \cdot \mathbf{u}_{s,f} \\ \sigma_{xs,f}(x,s,n) &= G \left(\boldsymbol{\phi}_{,s} \cdot \mathbf{u}_{x,f} + \boldsymbol{\psi} \cdot \mathbf{u}'_{s,f} \right) \end{aligned} \tag{14}$$

The linear stability analysis is performed by establishing the equilibrium equations on a deformed configuration within the vicinity of the fundamental path. By doing so, the existence of a bifurcation point, representing the intersection point between the fundamental and the secondary path, is ensured according to the adjacent equilibrium criterion, (Pignataro 1991).

Hence, the deformation of the thin-walled structure is defined by a configuration that is "disturbed" from the fundamental path through a small parameter (kinematically admissible). Considering the displacement field aproximation of Eqs. 5, the non-linear deformation of the thin-walled structure according to the hypotheses of (Novozhilov 1953) is given by

$$\begin{aligned} \delta\epsilon_x^{nl} &= \frac{\partial u_s}{\partial x}\frac{\partial \delta u_s}{\partial x} + \frac{\partial u_n}{\partial x}\frac{\partial \delta u_n}{\partial x} = \left(\boldsymbol{\psi}^t \mathbf{u}_{s,x}\right)\left(\boldsymbol{\psi}^t \, \partial \mathbf{u}_{s,x}\right) + \left(\boldsymbol{\chi}^t \mathbf{u}_{n,x}\right)\left(\boldsymbol{\chi}^t \partial \mathbf{u}_{n,x}\right) \\ \delta\epsilon_s^{nl} &= \frac{\partial u_s}{\partial s}\frac{\partial \delta u_s}{\partial s} + \frac{\partial u_n}{\partial s}\frac{\partial \delta u_n}{\partial s} = \left(\boldsymbol{\psi}_{,s}^t \mathbf{u}_s\right)\left(\boldsymbol{\psi}_{,s}^t \partial \mathbf{u}_s\right) + \left(\boldsymbol{\chi}_{,s}^t \mathbf{u}_n\right)\left(\boldsymbol{\chi}_{,s}^t \partial \mathbf{u}_n\right) \\ \delta\gamma_{xs}^{nl} &= \frac{1}{2}\left(\frac{\partial u_s}{\partial x}\frac{\partial \delta u_s}{\partial s} + \frac{\partial u_s}{\partial s}\frac{\partial \delta u_s}{\partial x} + \frac{\partial u_n}{\partial s}\frac{\partial \delta u_n}{\partial x} + \frac{\partial u_n}{\partial x}\frac{\partial \delta u_n}{\partial s}\right) = \left(\boldsymbol{\psi}^t \mathbf{u}_{s,x}\right)\left(\boldsymbol{\psi}_{,s}^t \partial \mathbf{u}_s\right) \\ &\quad + \left(\boldsymbol{\psi}_{,s}^t \mathbf{u}_s\right)\left(\boldsymbol{\psi}^t \partial \mathbf{u}_{s,x}\right) + \left(\boldsymbol{\chi}_{,s}^t \mathbf{u}_n\right)\left(\boldsymbol{\chi}^t \partial \mathbf{u}_{n,x}\right) + \left(\boldsymbol{\chi}^t \mathbf{u}_{n,x}\right)\left(\boldsymbol{\chi}_{,s}^t \partial \mathbf{u}_n\right) \end{aligned} \tag{15}$$

The first variation of the energy associated with the thin-walled structure is computed so as to derive the beam equilibrium equations. Hence, the stress field corresponding to the pre-buckling state as defined by Eqs. 14 is considered, being the corresponding variation of deformation obtained by adding to the deformation field given by Eq. 6 the non-linear terms defined in Eqs. 15. The higher order equilibrium equations of a thin-walled configuration that is "disturbed" from the fundamental path is therefore obtained by considering the contribution of the

corresponding non-linear geometric terms, in addition to the equilibrium equations, Eq.12, being written as follows,

$$\mathbb{K}_4\,\mathbf{u}'''' + \left(\mathbb{K}_2 - \mathbb{K}_2^G\right)\mathbf{u}'' + \left(\mathbb{K}_1 + \mathbb{K}_1^G\right)\mathbf{u}' + \mathbb{K}_0\,\mathbf{u} = 0 \tag{17}$$

where $\mathbb{K}_2^{G}$ and $\mathbb{K}_1^{G}$ are geometric matrices and are obtained according to the pre-buckling of the structure. Considering the structure subjected to in-plane membrane forces at both end sections, i.e., a state of stress defined by axial components of the stress field of Eq. 13, the matrix $\mathbb{K}_1^{G}$ results null, being $\mathbb{K}_2^{G}$ defined as follows:

$$\begin{gathered}
\mathbb{K}_2^G = \begin{bmatrix} \cdot & \cdot & \cdot \\ \cdot & \boldsymbol{\kappa}_x^1 & \cdot \\ \cdot & \cdot & \boldsymbol{\kappa}_x^2 \end{bmatrix} \\
\boldsymbol{\kappa}_x^1 = \boldsymbol{\kappa}_{xi}^1\, u'_{xi,f} \quad \text{with} \quad \kappa_{xi,jk}^1 = E^*\,t \int_\Gamma \phi_i\,\psi_j\,\chi_k\,ds \\
\boldsymbol{\kappa}_x^2 = \boldsymbol{\kappa}_{xi}^2\, u'_{xi,f} \quad \text{with} \quad \kappa_{xi,jk}^2 = E^*\,t \int_\Gamma \phi_i\,\chi_j\,\chi_k\,ds
\end{gathered} \tag{18}$$

The bifurcation loads and the corresponding buckling modes are obtained either from an analytical or a numerical solution of Eq. 17. To this end, the set of the equilibrium equations are written in the set of coordinates corresponding to the uncoupled modes derived from the eigenvalue problem. By doing so, the model's governing equations become uncoupled to the most possible form, yielding a set of beam-like equations. In the uncoupled form of the governing equations, some of the corresponding coefficient matrices have non-null components off the principal diagonal. These non-null components allow to identify the buckling modes of the structure as a linear combination of orthogonal displacement modes. The equilibrium equations of a buckling mode are therefore obtained by condensing the uncoupled form of equations Eq. 17 to the set of coordinates that corresponds to the displacement modes defining the buckling mode.

3. Examples of application

The local and global buckling of a thin-walled column with a rectangular hollow section is analyzed through the higher order beam model. The column is simply supported and subjected to a compressive uniform axial stress. Local and global bifurcation loads and the corresponding buckling modes are obtained analytically and numerically, being compared with the results of a shell finite element model implemented in ABAQUS.

The rectangular hollow section has a width b_f =100 mm, a height h_w =200mm and a wall thickness of 2 mm. The steel is considered to have an elastic modulus of 210 kN/mm^2, being the Poisson effect neglected and the cross-section walls admitted to be undeformable along the respective midline, i.e., ε_s =0. A cross-section analysis is performed by considering the rectangular hollow section divided into 4 elements as represented in Fig. 2, being the approximation of the displacement along each element defined by Eq. 5. Towards the definition of the structure's uncoupled deformation modes, the non-linear eigenvalue problem associated

with the beam governing equations is solved, being derived the in-plane orthogonal displacement modes represented in Fig. 3.

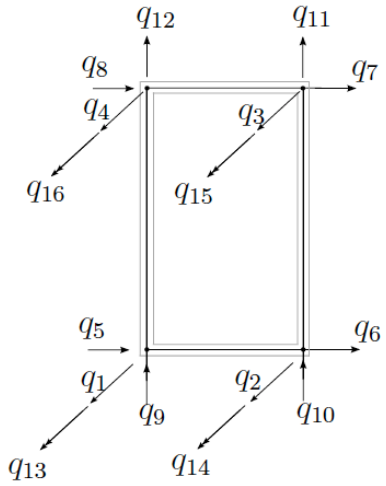

Figure 2: Rectangular hollow section discretization.

The beam governing equations are rewritten considering the displacement modes of Fig. 3, which allows to obtain a meaningful form of the equations, retrieving classic equations and put forward beam-like equations for higher order modes. The coupling between modes in the rewritten form of the equations allows to identify the displacement modes that should be considered on the definition of local and global buckling modes. The bifurcation loads are then obtained from the solution of the linear stability Eqs. 17 considering the linear combination of displacement modes that defines the corresponding buckling mode.

For the thin-walled column with the rectangular hollow cross-section, the following linear combinations of displacement modes are identified as local buckling modes: (i) $\mathbf{u}_{\text{LB1}}= \beta_2$; (ii) $\mathbf{u}_{\text{LB2}}= \{v,\ \beta_3\}$; (iii) $\mathbf{u}_{\text{LB3}}= \{w,\ \beta_4\}$. In-plane flexural displacement modes β_2, β_3 and β_4 are represented in Fig. 3 and were obtained from the eigenvalue problem of the higher order beam model.

The bifurcation load of the buckling mode $\mathbf{u}_{\text{LB1}}$ is obtained by condensing the equilibrium equations to the displacement mode β_2, which can be written as follows,

$$E^* \, k_4^{\beta_2,\beta_2} \, \beta_2'''' \, + \, G \, k_2^{\beta_2,\beta_2} \, \beta_2'' \, + \, E^* \, k_0^{\beta_2,\beta_2} \, \beta_2 \, - \, \lambda_\sigma \, k_g^{\beta_2,\beta_2} \, = \, 0 \tag{19}$$

The bifurcation load associated with buckling mode $\mathbf{u}_{\text{LB1}}$ is obtained analytically by considering a sinusoidal solution of Eq. 5, being the corresponding results for several column lengths and different wavelengths depicted in Fig. 4. Consider now for the thin-walled column the buckling mode $\mathbf{u}_{\text{LB2}}$, which is given as a combination of the in-plane flexural displacement mode β_3 and the transverse displacement v. Condensing the linear stability equations to v and β_3 and considering a solution of the form,

$$\mathbf{u}_{LB_2} \, = \, \sin\left(\frac{m \, \pi \, x}{L}\right) \, \left[\begin{array}{cc} v_0 & \beta_{3,0} \end{array} \right]^T \tag{20}$$

allows to evaluate the bifurcation load of mode $\mathbf{u}_{LB2}$, which is represented in Fig. 5. for several column lengths.

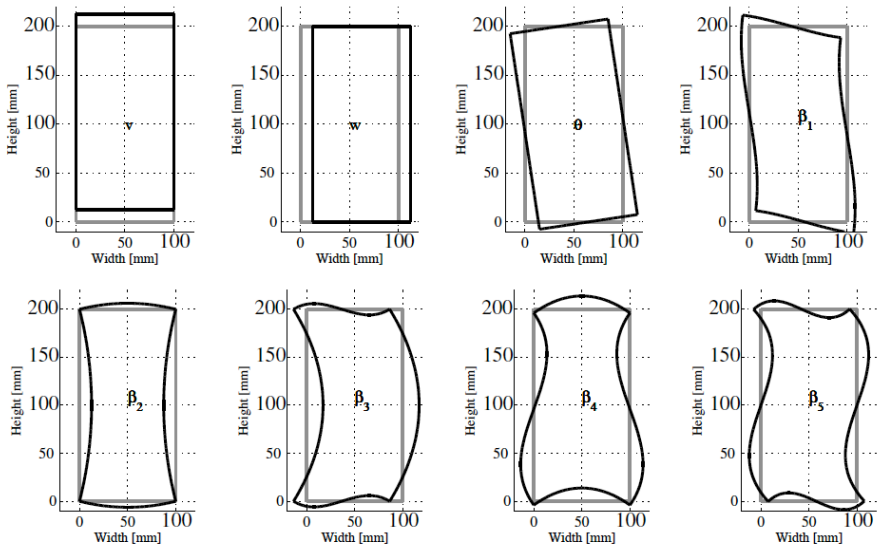

Figure 3: Rectangular hollow section displacement modes.

The bifurcation loads of the global buckling modes can also be obtained from the higher order model by considering appropriate displacement modes combination. To this end, the following combinations can be considered: $\mathbf{u} = \{\theta_z, v\}$ for the flexural buckling around the z axis; $\mathbf{u} = \{\theta_y, w\}$ for the flexural buckling around the y axis; $\mathbf{u} = \{\theta, \omega\}$ for the torsional buckling.

Admitting a possible interaction with the global buckling mode that corresponds to the flexure around the y axis, it is possible to obtain an analytical solution that considers equal wavelengths for all the displacement modes involved. The buckling mode is then defined as follows,

$$\mathbf{u}_{LB_2} = \left[\begin{array}{ccc} v(x) & \theta_y(x) & \beta_3(x) \end{array} \right]^t \tag{21}$$

being considered the following analytical solution,

$$\mathbf{u}_{LB_2} = \left[\begin{array}{c} v_0 \, \sin\left(m\,\pi\,x/L\right) \\ \theta_z \, \cos\left(m\,\pi\,x/L\right) \\ \beta_{3,0} \, \sin\left(m\,\pi\,x/L\right) \end{array} \right] \tag{22}$$

The bifurcation loads associated with buckling mode $\mathbf{u}_{LB2}$, the global flexural buckling and the interaction between local and global modes is represented for several lengths in Fig. 6.

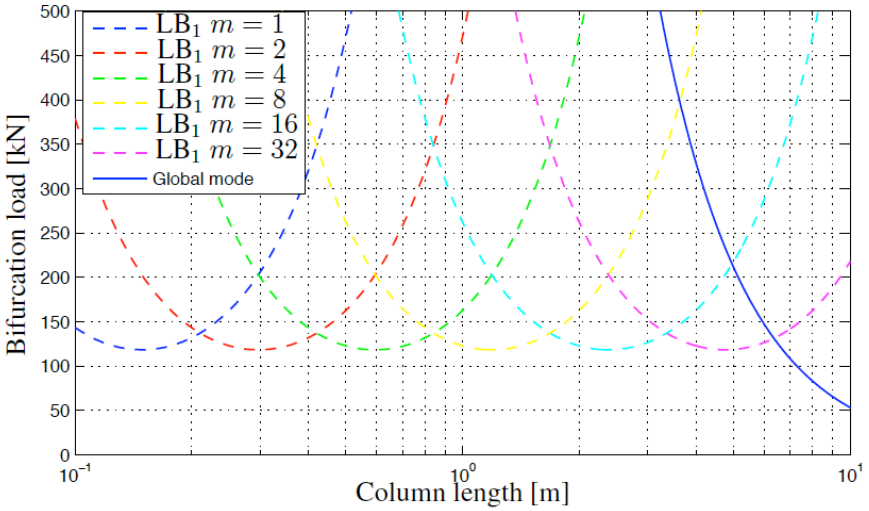

Figure 4: Global-local ($\mathbf{u}_{\mathrm{LB1}}$) bifurcation loads, rectangular hollow section.

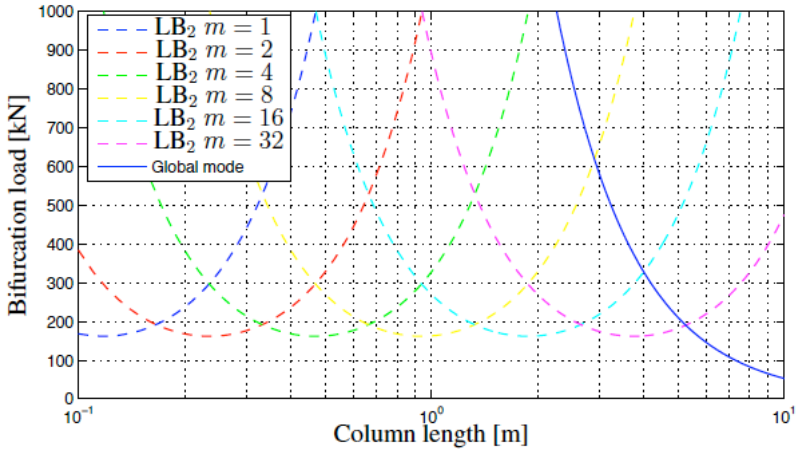

Figure 5: Global-local ($\mathbf{u}_{\mathrm{LB2}}$) bifurcation loads, rectangular hollow section.

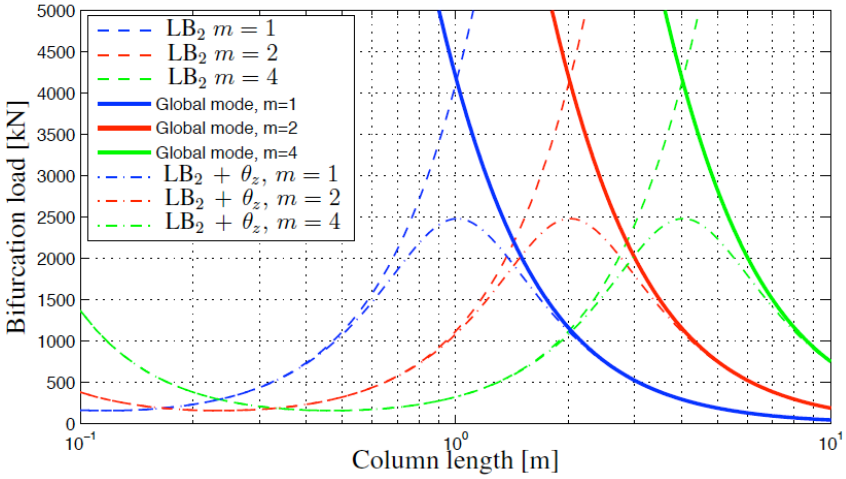

Figure 6: Interaction between global and local modes, rectangular hollow section.

A numerical solution of the linear stability analysis through the finite element method is considered. The formulation considers the approximation of the uncoupled displacement modes along the finite element by a set of interpolation functions, deriving a weak form of Eq. 17. The numerical formulation has the advantage of allowing to verify whether the local and buckling modes interact without being limited to consider modes with the same wavelength.

The following boundary conditions were considered for the finite element model: (i) both transverse displacements prevented at both end sections; (ii) the axial displacement fixed in one end section; (iii) the torsional rotation fixed in one end section; and (iv) the modes associated with in-plane modes blocked at both end sections. The bifurcation loads obtained for several column lengths are represented in Fig. 7 where the bifurcation loads obtained analytically for the most relevant mode, β_2, are compared with the bifurcation loads obtained numerically through the developed model (considering all the cross section displacement modes) for a mesh of 8 and 32 finite elements lengthwise. The numerical and analytical results are in a good agreement except for the column length range 3000mm to 4000mm, where the numerical model with 8 finite elements it is not sufficiently refined to capture the local buckling of the column. However, for the more refined model of 32 elements this issue no longer occurs.

A model of a three dimensional mesh of shell elements considering a division of 16 × 60 elements in the transverse section and in the column length, respectively, was implemented in ABAQUS, in order to verify the accuracy of the results obtained from the higher order beam model. The bifurcation loads obtained from ABAQUS are also represented in Fig. 7, showing a good agreement with the numerical results obtained through the one-dimensional finite element.

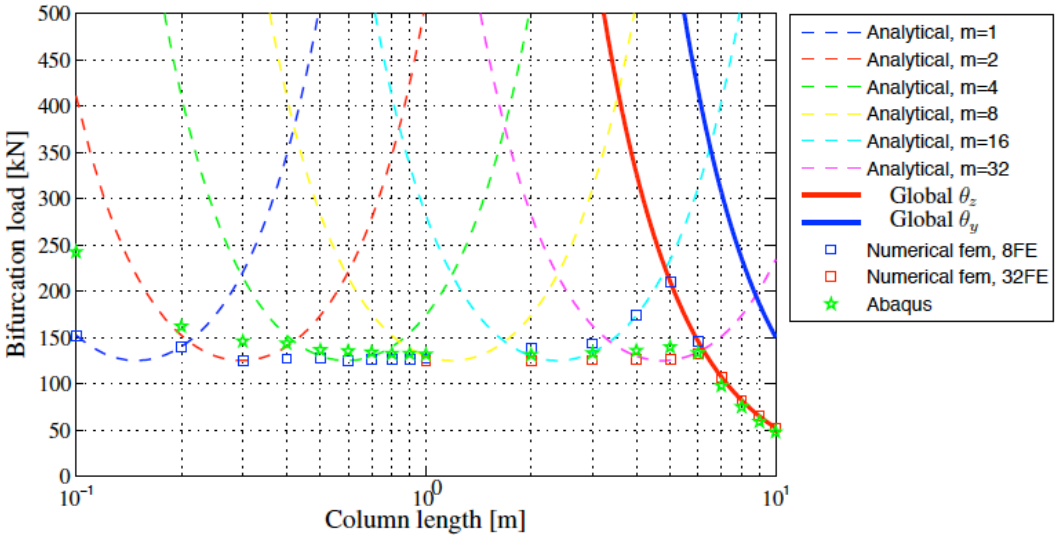

Figure 7: Global-local bifurcation loads, comparison with a shell model.

The buckling mode obtained from the developed finite element model for a column of L=1000 mm is plotted in Fig. 8 where it can be verified that the in-plane shape of the buckling mode corresponds to β_2 and the number of wavelengths is in agreement with the analytical formulation. Notice that the Fig. 8 corresponds to a one-dimensional model, i.e., only the amplitudes of the

displacement modes were interpolated along the beam axis; hence, the apparent mesh depicted in the figure is only of a post-processed nature.

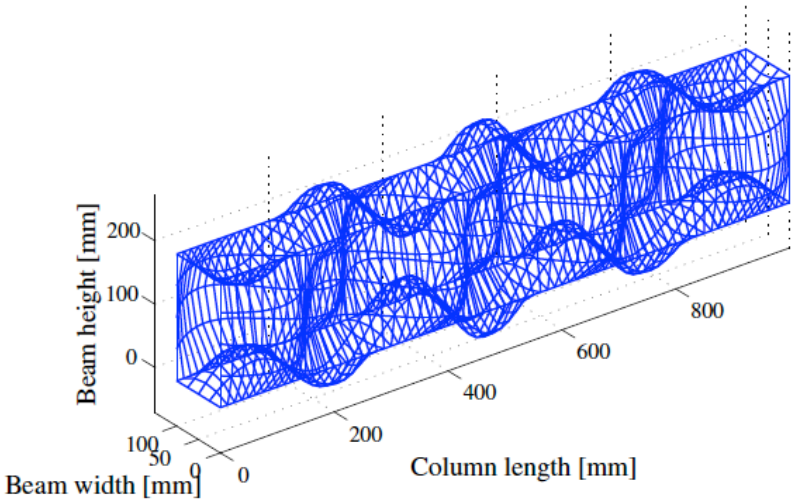

Figure 8: Column buckling mode.

A simply supported column with an I shaped cross-section with an elastic modulus of 210 kN/mm^2 is herein also considered for a linear stability analysis so as to shed a light on the corresponding buckling phenomena. The cross-section has a web with dimensions 1200 mm ×10 mm and two equal flanges of dimensions 600 mm × 25 mm. The cross-section analysis is performed considering a discretization with 5 elements as represented in Fig. 9. The tangential deformability along the profile midline is restricted and therefore the 22 initial degrees of freedom are reduced to a total of 19 degrees of freedom for the cross section.

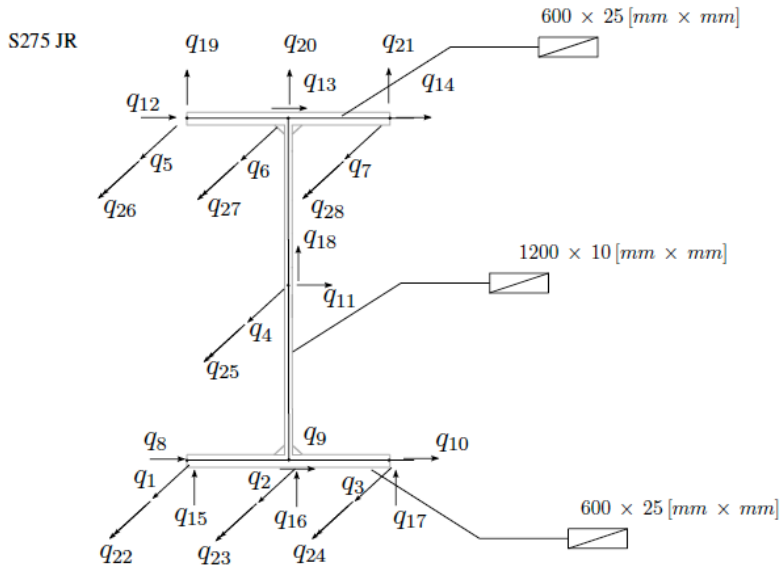

Figure 9: I shaped cross-section discretization.

The two most significant higher order modes β_1 and β_2 are represented in Fig. 10.

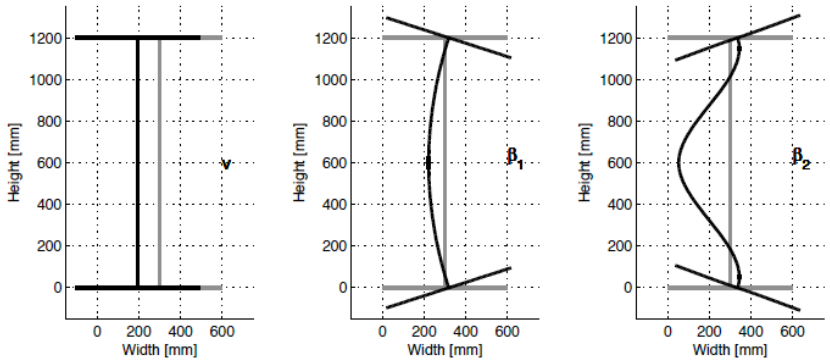

Figure 10:I shaped cross-section, in-plane modes.

The local buckling mode of the column can be defined as follows,

$$\mathbf{u}_{LB_1} = \left[\begin{array}{ccc} v(x) & \beta_1(x) & \beta_2(x) \end{array} \right]^t \tag{23}$$

being the corresponding linear stability equations obtained by condensing the governing equations to these modes,

$$E^* \, \mathbf{K}_{4,LB_1} \, \mathbf{u}''''_{LB_1} + G \, \mathbf{K}_{2,LB_1} \, \mathbf{u}''_{LB_1} + E^* \, \mathbf{K}_{0,LB_1} \, \mathbf{u}_{LB_1} - P/A \, \mathbf{K}_{G,LB_1} \, \mathbf{u}''_{LB_1} = 0 \tag{24}$$

A linear eigenvalue problem is obtained by considering the following solution,

$$\mathbf{u}_{LB_1} = \sin\left(\frac{m \, \pi \, x}{L}\right) \left[\begin{array}{ccc} v_0 & \beta_{1,0} & \beta_{2,0} \end{array} \right]^T \tag{25}$$

which allows to determine the corresponding bifurcation loads for several half-length waves; the results are represented in Fig. 11. The minimum bifurcation load obtained for the local buckling is almost a constant value for different half-lengths with different column lengths, $P_{cr} \cong 3470$kN.

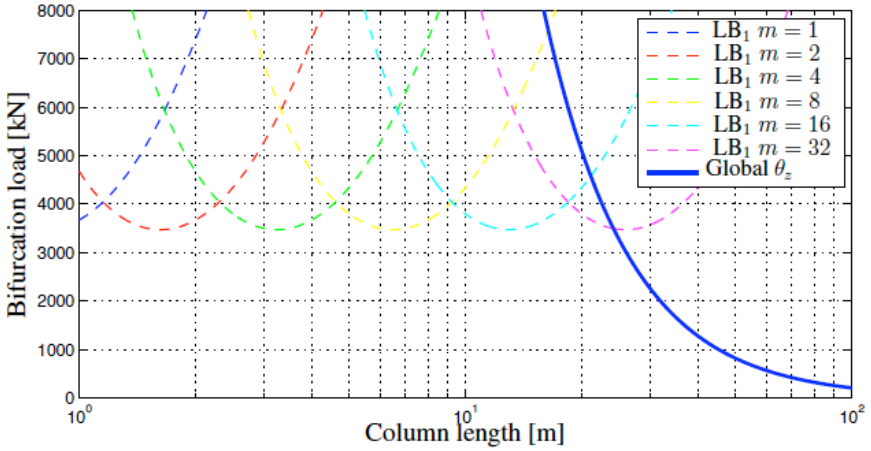

Figure 11: Global-local bifurcation loads, I shaped cross-section.

Considering the buckling mode defined only as a linear combination of the transverse displacement v and the distortional mode β_1, the corresponding bifurcation load would be several times higher than the one obtained by adopting the buckling mode defined in Eq. 23. In fact, the

buckling of this column, given the slenderness of the corresponding web and flanges, is essentially governed by the web buckling, as it can be verified in (Allen 1980) and hence the results would be sensitive to the flexural web stiffness.

The buckling analysis that considers the interaction between the local and the flexural mode that corresponds to the rotation around the y axis is performed by considering the following displacement modes,

$$\mathbf{u}_{FL+LB_1} = \left[\theta_y(x) \quad v(x) \quad \beta_1(x) \quad \beta_2(x) \right]^T \tag{26}$$

The bifurcation loads considering the interaction of flexural and local buckling modes were obtained by considering a solution of the following form,

$$\begin{aligned} \theta_y(x) &= \theta_{y0} \cos(k\,x) & v(x) &= v_0 \sin(k\,x) \\ \beta_2(x) &= \beta_{2,0}(x) \sin(k\,x) & \beta_3(x) &= \beta_{3,0}(x) \sin(k\,x) \end{aligned} \tag{27}$$

being represented in Fig. 12 for several column lengths.

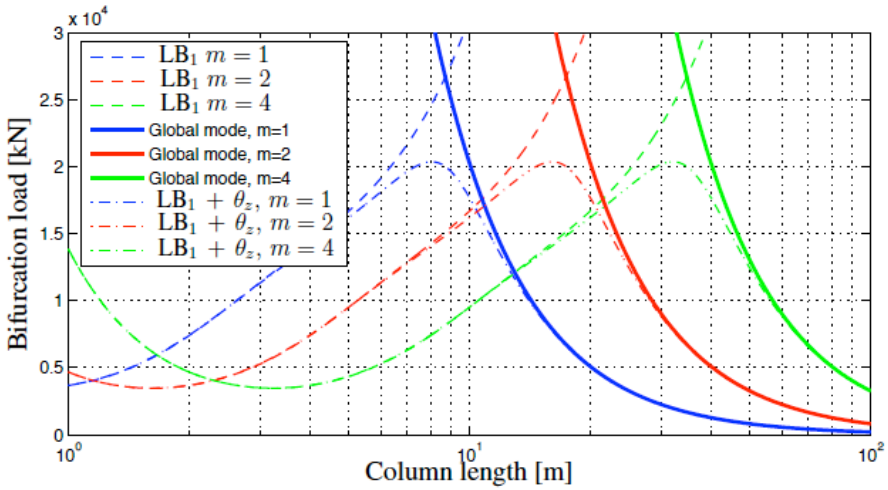

Figure 12: Interaction between global and local modes, I shaped cross-section.

The bifurcation loads obtained by the higher order beam model both numerically (through the developed one dimensional finite element model) and analytically are compared with the results obtained from a shell model implemented in ABAQUS in Fig. 13, allowing to conclude good agreement of results. The buckling mode obtained from the one-dimensional finite element model is represented for a column length of 3000mm and 8000mm in Figs. 14 and 15 respectively. A good agreement between the results from the shell and the higher order beam model regarding the number of wavelengths associated with the buckling modes was also obtained.

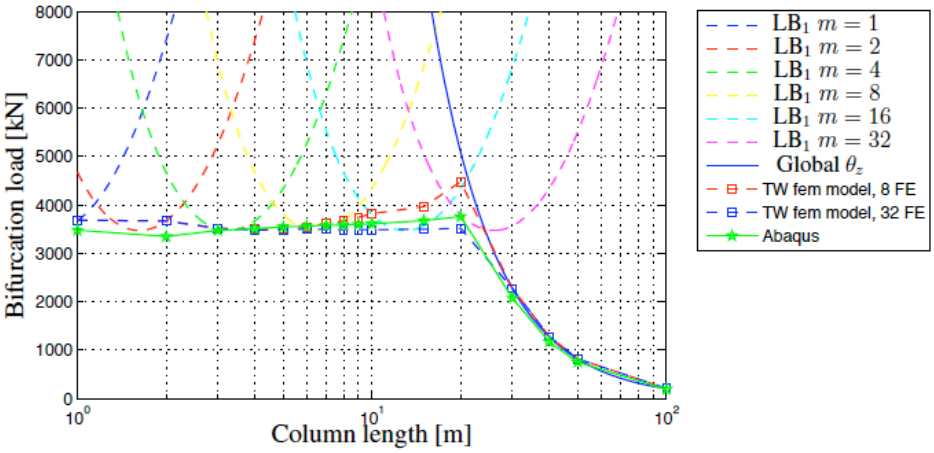

Figure 13: Global-local bifurcation loads, comparison with a shell model.

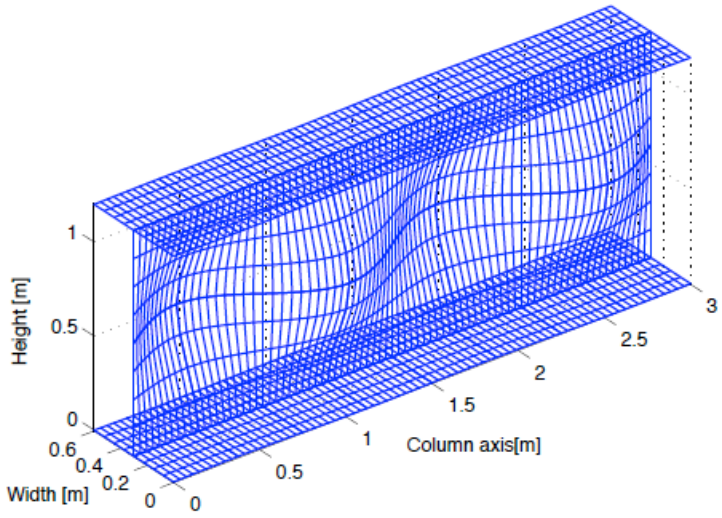

Figure 14: Buckling mode (beam model), L=3000mm.

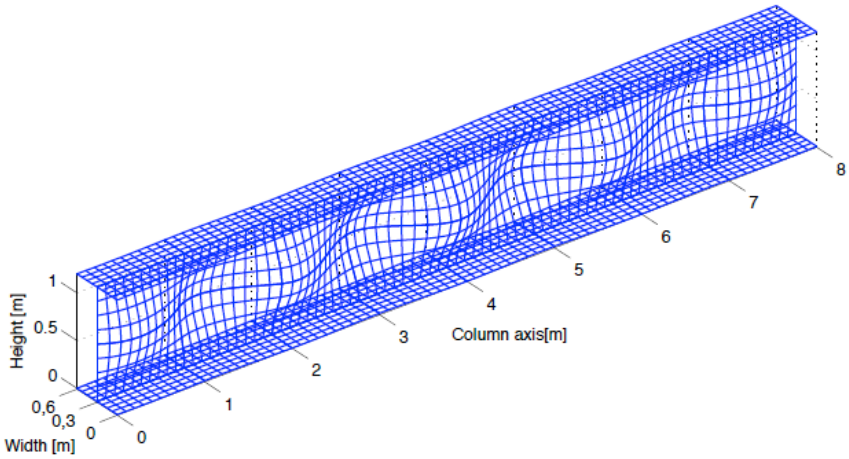

Figure 15: Buckling mode (beam model), L=8000mm.

4. Conclusions

The basis of a higher order beam model for the analysis of thin-walled structures was presented. The model relies on the approximation of the displacement field over the cross-section in order to adequately represent the three-dimensional structural behaviour and on a consistent criterion for the definition of uncoupled modes. The uncoupled nature of the model has allowed to derive sets of beam-like equations representing classic deformations and local effects.

Local and global buckling phenomena were successfully analysed through the higher order beam model. In fact, since the beam model considers the in-plane flexure of the cross-section, it can efficiently consider local buckling. Moreover, the definition of uncoupled modes enhances the perception of stability phenomena by identifying the relevant structural behaviour. Towards the definition of bifurcation loads and the corresponding buckling loads, a linear stability analysis was performed by considering a linear pre-buckling state and employing the adjacent equilibrium criterion. The governing equations were written for the vicinity of the fundamental path considering the displacement modes in the uncoupled form.

Two approaches were considered for the solution of the linear stability equations: (i) an analytical solution considering a trigonometric lengthwise variation of the mode and (ii) a numerical solution cast within the finite element method. The analytical solution has allowed to define for each buckling mode the corresponding bifurcation load, being nevertheless limited to consider an equal wavelength for local and global buckling modes. Therefore, the analytical formulation was not adequate to consider the interaction between modes. To this end, the numerical model has proven to be efficient in as much as it considers the adequate wavelength of each mode by a proper refinement of the finite element mesh in order to define a solution of the problem.

A shell finite element model implemented in ABAQUS was also adopted, being the corresponding results in terms of bifurcation loads and the respective buckling modes in an excellent agreement with the results obtained from the higher-order beam model.

References

Ádány, S., Schafer, B.W. (2008). "A full modal decomposition of thin-walled, single-branched open cross-section members via the constrained finite strip method". *Journal of Constructional Steel Research* 64(1), 12–29.

Ádány, S., Silvestre, N., Schafer, B.W., Camotim, D. (2009). "GBT and cFSM: Two modal approaches to the buckling analysis of unbranched thin-walled members. *International Journal of Advanced Steel Construction* 5(2), 195-223.

Allen, H. G. and Bulson, P. S. (1980). Background to buckling. McGraw-Hill.

Andreassen, M. J. and Jonsson, J. (2013). "A distortional semi-discretized thin-walled beam element". *Thin-Walled Structures* 62 (4), 142–157.

Carrera, E. Giunta, G. Petrolo, M. Beam Structures: Classical and Advanced Theories. John Wiley and Sons Ltd, 2011.

Carrera, E. Giunta, G. (2010). "Refined beam theories based on a unified formulation". *International Journal of Applied Mechanics and Engineering*, vol. 2, 117- 143.

Dinis, P., Camotim, D., Silvestre, N. (2006). "GBT formulation to analyse the buckling behaviour of thin-walled members with arbitrarily branched open cross-sections". *Thin-Walled Structures* 44 (1), 20–38.

Fatmi, R. E. (2007). “Non-uniform warping including the effects of torsion and shear forces”. part i: A general beam theory. *International Journal of Solids and Structures* 44 (18-19), 5912–5929.

Ferradi, M. K. Cespedes, X. Arquier, M. (2013(. “A higher order beam finite element with warping eigenmodes”. *Engineering Structures*, Vol. 46: 748-762.

Ferradi, M.K. Cespedes, X. (2014). “A higher order beam finite element with warping eigenmodes”. *Computers and Structures*, Vol. 131 (15): 12-33.

Genoese, A. Genoese, A. Bilotta, A. and Garcea, G. (2013). “A mixed beam model with non-uniform warpings derived from the Saint-Venant rod”. *Computers and Structures*, Vol. 121: 87-98.

Genoese, A. Genoese, A. Bilotta, A. and Garcea, G. (2014). “A generalized model for heterogeneous and anisotropic beams including section distortions”. *Thin-Walled Structures*,Vol. 74: 85-103.

Genoese, A. Genoese, A. Bilotta, A. and Garcea, G. (2014). “A composite beam model including variable warping effects derived from a generalized Saint Venant solution”. *Composite Structures*, Vol. 110: 140-151.

Genoese, A. Genoese, A. Bilotta, A. and Garcea, G. (2014). “A geometrically exact beam model with non-uniform warping coherently derived from the Saint Venant rod”. *Engineering Structures*, Vol. 68 (1): 33-46.

Gonçalves, R., Dinis, P. B., Camotim, D. (2009). “GBT formulation to analyse the first-order and buckling behaviour of thin-walled members with arbitrary cross-sections”. *Thin-Walled Structures* 47, 583–600.

Hodges, D., 2006. Non-linear composite beam theory. AIAA.

Jonsson, J. and Andreassen, M.J. (2011). “Distortional eigenmodes and homogeneous solutions for semi-discretized thin-walled beams”. *Thin-Walled Structures* 49 (6), 691–707.

Kim, J. H., Kim, Y. Y., (1999). “Analysis of thin-walled closed beams with general quadrilateral cross sections” *Journal of Applied Mechanics*, Vol. 66: 904-912.

Kim, J. H., Kim, Y. Y., (2000). “One dimensional analysis of thin-walled closed beams having general cross-sections”. *International Journal For Numerical Methods in Engineering* 49, 653–668.

Kim, Y. Y., Kim, Y., (2002). “A one-dimensional theory of thin-walled curved rectangular box beams under torsion and out-of-plane bending”. *International Journal for Numerical Methods in Engineering* 53, 1675–1693.

Li, Z., Hanna M.T., Ádány, S., Schafer, B.W. (2011). “Impact of basis, orthogonalization, and normalization on the constrained Finite Strip Method for stability solutions of open thin-walled members”. *Thin-Walled Structures* 49(9), 1108– 1122.

Nedelcu, M. (2010). “GBT formulation to analyse the behaviour of thin-walled members with variable cross-section”. *Thin-Walled Structures*, Vol. 48:629-638.

Novozhilov, V. V. (1953). Foundations of the Nonlinear theory of Elasticity. Graylock Press, Rochester - New York

Pavazza, R. Blagojevic´, B., 2005. “On the cross-section distortion of thin-walled beams with multi-cell cross-sections subjected to bending”. *International Journal of Solids and Structures* 42 (3-4), 901–925.

Piccardo, G. Ranzi, G. Luongo, A. (2014). “A direct approach for the evaluation of the conventional modes within the GBT formulation”. *Thin-Walled Structures*, Vol. 74:133-145.

Prokic, A. (1996). “New warping function for thin-walled beams. I: – theory”. *Journal of structural engineering*, Vol. 122(12):1437-1441.

Prokic, A., (1996). “New warping function for thin-walled beams. ii: Finite element method and applications”. *Journal of structural engineering*, Vol. 122(12):1443- 1452.

Razaqpur, A., Li,H. (1994). “Refined analysis of curved thin-walled multicell box-girder”. *Computers and Structures*, Vol. 53(1): 131-142.

Saadé, K., Warzée, G., Espion, B. (2006). “Modeling distortional shear in thin-walled elastic beams. *Thin-Walled Structures* 44, 808–821.

Schardt, R., (1989). Verallgemeinerte Technische Biegertheorie. Springer-Verlag, (in German).

Vieira, R. F., Virtuoso, F. and Pereira, E. B. R. (2013) “A higher order thin-walled beam model including warping and shear modes”. *International Journal of Mechanical Sciences*, 66, 67-82.

Vieira, R. F., Virtuoso, F. and Pereira, E. B. R. (2014) “A higher order model for thin-walled structures with deformable cross-sections”. *International Journal of Solids and Structure*, 51(3-4): 575-598.

Vieira, R. F., Virtuoso, F. B. E and Pereira, E. B. R. (2015) “Definition of warping modes within the context of a higher order thin-walled beam model”. *Computers and Structures* 147: 68-78.

Yu, W., Hodges, D. H. and Ho, J. C., (2012). “Variational asymptotic beam sectional analysis – An updated version”. *International Journal of Engineering Science*, 44(11-12), 3738-3755.